

THE CIRCUMSTELLAR MEDIUM AROUND EVOLVED MASSIVE STARS

JOSÉ RICARDO RIZZO

Universidad Europea de Madrid, E-28670 Villaviciosa de Odón, SPAIN

ELENA ORTIZ GARCÍA

Universidad San Pablo-CEU, E-28668 Boadilla del Monte, SPAIN

FRANCISCO M. JIMÉNEZ-ESTEBAN

Hamburger Sternwarte, Gojenbergsweg 112, D-21029 GERMANY

Abstract: The interplay between evolved massive stars (e.g., Of, B[e], red supergiant, luminous blue variable) and their surroundings is one of the less known issues in galactic astrophysics. In this article we report the first results of an observational campaign aiming to shed light on the evolution of the molecular gas as a consequence of massive star evolution. These results are presented in the form of maps ($4' \times 4'$ of maximum size), corresponding to the mm- and submm-wavelengths transitions of CO and ^{13}CO . Most of the observations were performed using the 10 m SMT radiotelescope at Arizona. We have detected tens of M_{\odot} of molecular gas, surrounding already known optical/IR nebula of ionized gas and warm dust. This molecular gas seems to be compressed in some parts, up to densities of several 10^4 cm^{-3} , probably by the action of strong and variable stellar winds and mass ejections. The CO opacity is also variable within a given field. These promising first results encourage both the study of new regions and the search for more complex molecular species in selected parts of these particular scenarios.

1 Introduction

From the very beginning of their formation process, massive stars are those objects which act most quickly and violently upon the surrounding gas and dust. Massive stars are formed after the collapse of giant molecular clouds, and later contribute with processed material to the interstellar medium during each evolutive phase. So far, the signposts provided by the stars in their environments are crucial in the understanding of star formation and evolution. Additionally, some stellar properties –such as, for example, the clumpiness of the winds– may

potentially be inferred from the study of the stellar outskirts. Finally, some high energy events, such as X-ray emission and gamma-ray bursts, are closely connected to the massive star evolution, previous to supernova.

Soon after their formation, massive stars are characterized by high mass-loss rates in the form of powerful stellar winds, and by strong UV radiation fields beyond the Lyman continuum limit. While massive stars are in the main sequence, these physical agents rapidly blow out an HII region, followed by large (several pc), expanding interstellar bubbles [1] which rapidly erode the natal molecular cloud [2], by means of their own expansion, shocks and photodissociation.

According to current evolutionary models, massive stars ($M > 25 M_{\odot}$) evolve off the main sequence, through Red Super Giant (RSG), then Luminous Blue Variable (LBV), and subsequently Wolf-Rayet (W-R), before exploding as supernova [3]. Under yet unclear circumstances, some stars may avoid the RSG stage. Main sequence lasts some 10^6 yr, while W-R spend few 10^5 yr. The pre-WR stages typically last from 10^3 yr to several 10^4 yr, and include several spectroscopic-characterized features (O(f), B[e], etc.). During each evolutive stage the stellar luminosity remains almost constant, although the wind features change appreciably, affecting the stellar environment. Several shockfronts are predicted [4, 5], which often are detected as neutral layers once cooled down. These layers would be located at different distances from the progenitor star, and may reach densities high enough to form new simple molecules. Related to the main sequence, several HI bubbles have been detected (see, for example [6, 7]); on the other hand, mid- and far-IR observations [8] have revealed the presence of warm dust associated to the RSG phase. Until recent years, the gas linked to the W-R stage has only been observed by the ionized W-R ring nebulae [9].

Traditionally, our observational knowledge about the ISM associated to every evolutive stage has been constrained to the UV and the optical windows. The neutral phase of the gas, both atomic and molecular, is being observed since the late 90's. The first detections of CO and H₂ around W-R nebulae [10, 11, 12] have proven that a significant fraction of the parent molecular cloud can survive the whole evolutive history of a massive star. The detection of ammonia [13] and other complex molecules [14] in NGC 2359 show that this molecular gas has been affected by moderate shocks and partially dissociated by the UV field from the star. Subsequent observations of CO, ¹³CO and C¹⁸O, with higher sensitivity and angular resolution [15], have revealed the presence of several shockfronts, related to evolutive phases *previous* to Wolf-Rayet.

These stages turn out to be the shortest lived (less than 10^5 yr), those which have the strongest winds (up to $10^{-4} M_{\odot} \text{ yr}^{-1}$), an important UV field (up to 10^6 times the mean interstellar UV field), and violent mass ejections (the LBV η Carina is the paradigm of the evolved massive stars). These conditions favour

the formation of warm/hot dust, circumstellar disks and shocked regions. The observational study of these evolutive signatures has been exclusively limited to the hot dust, which emits mainly in the mid-IR [16, 17, 18, 19].

Our work focusses primarily on the detection of molecular gas in the outskirts of post-main-sequence stars. The initial sample contains objects of several spectral types such as O(f), OIII, B[e], RSG, LBV, LBV-candidates and Wolf-Rayet. Around most of these stars, there have been previously identified bright nebulae, studied from the optical to the mid-IR. In all the cases analyzed, nebulae, disks and tori have a stellar origin, and it is striking how little is known about the pre-existing material, or how it was affected by these evolved stages. In this sense, the detection and follow-up study of the molecular gas is revealed as a powerful observational tool.

This essay reports for the first time the presence of molecular gas surrounding evolved massive stars previous to W-R, by the millimeter and sub-millimeter observations of CO and its isotopes. As we will show below, the molecular gas remains moderately dense (up to several $\sim 10^5 \text{ cm}^{-3}$) and warm (higher than 50 K), and is located beyond the ionized gas. The heating of the gas may have been produced by moderate shocks, provided by the strong enhancement discovered in some small regions. These relatively warm and dense regions constitute a new scenery of study, potentially significant in the chemical and dynamical evolution of the Galaxy.

2 Observational data

The observations were carried out using the 10 m SMT radiotelescope at Mt. Graham, operated by the Arizona Radio Observatory. The rotational transitions CO $2 \rightarrow 1$ (230.538 GHz), CO $3 \rightarrow 2$ (345.796 GHz), and the ^{13}CO $2 \rightarrow 1$ (220.398 GHz) lines were observed. The angular resolution (HPBW) was $36''$ and $24''$ at 1.3 mm and 0.8 mm, respectively.

Two-channel receivers were employed, connected to acoustic-optical spectrometers and filter banks; with this equipment, velocity resolutions between 0.6 and 2.1 km s^{-1} were achieved. Calibration was done by observing standard line calibrators. Pointing and focus were checked every 2 and 6 hours, respectively.

In most cases, several fields $3'-4'$ wide were observed by using the *on-the-fly* (OTF) technique. In some cases, the low S/N ratio attained with single maps made mandatory the average of several OTF maps, performed in orthogonal directions. For sources of small size, a few positions towards the center and the close vicinity were observed in position-switching mode.

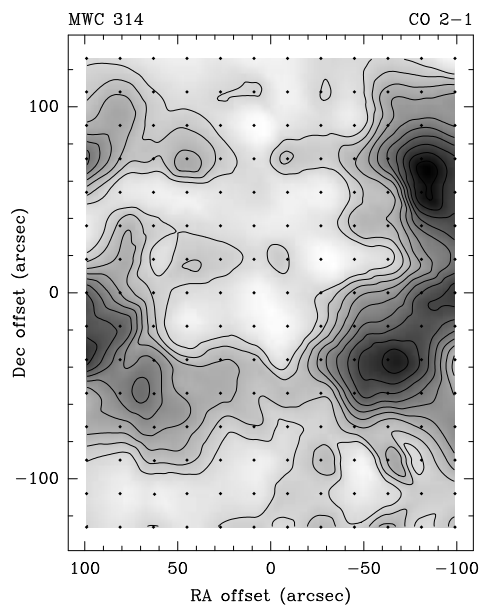


Figure 1: CO 2–1 emission map in the field of MWC 314. Starting contours and steps are 0.8 K km s^{-1} .

3 Results

3.1 Overall

The OTF technique has proved to be an adequate tool in order to detect and subsequently analyze the molecular gas around our sample stars. In most of the cases, the detection was positive, although we have achieved reasonable high S/N ratio in a handful of objects. In the case of sources which have extended optical/IR nebular emission, it was found that the CO bounds the nebulae, resembling the case of NGC 2359 [15]. As an example, Figure 1 shows the distribution of the CO 2–1 around the B[e] star MWC 314 (also recognized as an LBV candidate [20]).

In the case of sources with smaller circumstellar disks, impossible to resolve with our telescope, we pointed toward the target stars and a few positions around them; in these cases, we could isolate kinematic components from the general ones, which will be further analyzed.

In the following, we shall briefly describe the results obtained toward two of our best studied sources: G79.29+0.46 and NGC 7635.

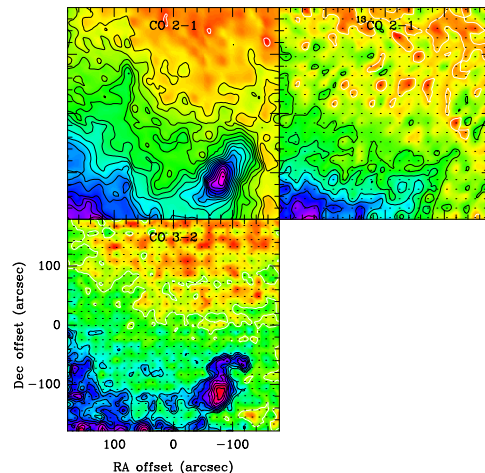


Figure 2: Molecular gas distribution around G79.29+0.46. Lines are indicated in the top center of each map. Starting contours and steps are: 3 and 1 K km s^{-1} for CO 2–1; 2 and 1 K km s^{-1} for ^{13}CO 2–1; 8 and 2 K km s^{-1} for CO 3–2. It is possible to note different spatial distribution of the lines: while the 2–1 lines are widespread all along the field, the CO 3–2 lines is mainly concentrated to the southern part of the mapped area.

3.2 G79.29+0.46

G79.29+0.46 was firstly identified as a continuum source, and later recognized as a ring nebula around a hot star [21]. The exciting star is now confirmed as a very luminous LBV ($L_* > 10^5 L_\odot$; [22]). The ring nebula is probably made of ejected gas, has a mass of $14 M_\odot$ and a dust temperature around 70 K [23].

In Figure 2 we show a panel of three maps sketching the distribution of CO 2–1, ^{13}CO 2–1, and CO 3–2 lines. The CO and ^{13}CO 2–1 maps show a widespread distribution, but preferably concentrated to the southwest, probably associated to the Cyg X region [21]. Interestingly, the CO 3–2 line appears much more concentrated in a circular “layer”, less than 40” width.

In Figure 3 (left panel) we can see the distribution of the CO 3–2 emission superimposed onto an ISO image at $25\mu\text{m}$. CO is clearly bounding the ring nebula, which is consistent with the hypothesis of a previous mass ejection followed by gas compression by non-dissociative shocks. The higher critical density of the

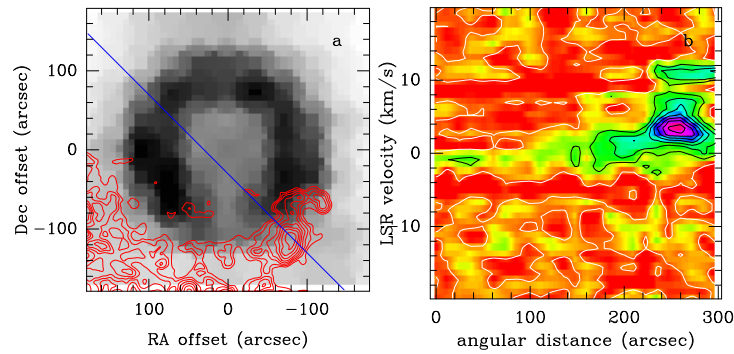


Figure 3: (a) CO 3–2 emission map in the field of G79.29+0.46, superimposed to an ISO image at $25\ \mu\text{m}$. (b) A position-velocity map of the CO 3–2 line, traced along the strip sketched in Figure a. The strip direction is 45 degrees (east to north). The notably enhanced emission (up to 14 km/s) corresponds to the southeastern feature clearly seen in Figure a.

CO 3–2 line ($\sim 2 \cdot 10^4\ \text{cm}^{-3}$), compared with the other lines, strengthens this hypothesis.

Specially striking is the southeast clump at $\sim (-80'', -110'')$. Figure 3 (right panel) shows a position-velocity map taken at a diagonal NE-SW slice. We can clearly see a sudden enhancement, and a change in CO velocities, when the slice crosses the clump. There, the linewidth is $14\text{--}16\ \text{km s}^{-1}$, an unusual amount in quiescent clouds. Both the large linewidth and their small angular scale tell us about the presence of a shock acting upon the clump. Physical parameters may even be more extreme within the clump, and should deserve further observations of higher-excitation lines.

3.3 NGC 7635

NGC 7635 (also known as “The Bubble Nebula”) is an optical nebula excited by the O-giant BD+60 2522 [24]. It is also immersed within the diffuse nebula S 162, excited by Cas OB2 [25].

Figure 4 shows the distribution of the CO 2–1 (left) and the CO 3–2 (right). In both cases we can see a morphology closely similar to G79.29+0.46. We have also identified particular positions toward the northern and western parts of the map, which may be related to shocks and will be further analyzed by follow-up observations.

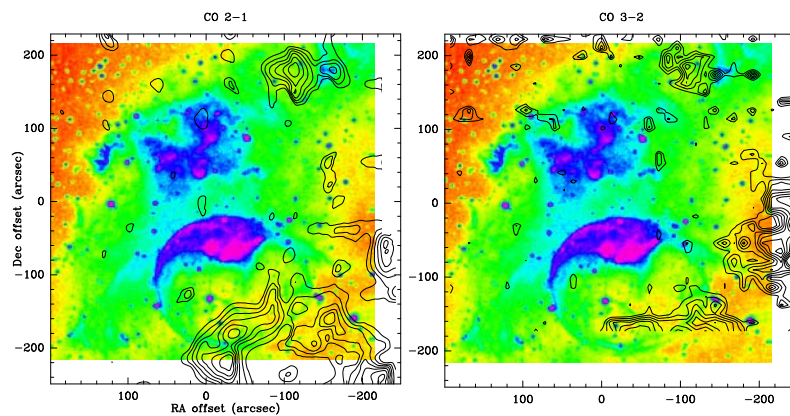


Figure 4: CO 2–1 (left) and 3–2 (right) emission maps in the field of NGC 7635. The CO emission is shown by contours, superimposed to a false-colour R-image of the nebula, also known as “The Bubble Nebula”.

4 Physical parameters

This multi-line study allows us to crudely estimate some global parameters, such as the mass, mean density and opacity of the CO lines. To derive the mass, we have integrated the emission in a given area, and assumed LTE and an excitation temperature of 20 K. An LVG code, which assumes non-LTE conditions and emitting volumes proportional to the linewidths, was used to roughly estimate the density and opacity of the lines. By this second method, we get higher column densities, and therefore the masses should be considered as lower limits. Table 1 summarizes the achieved results.

Source	Mass M_{\odot}	Mean density cm^{-3}	Max density cm^{-3}	τ_{21} at max
G79.29+0.46	60	700	$> 3 \cdot 10^4$	2
NGC 7635	40	500	$> 10^4$	1

Table 1: Global CO parameters in G79.29+0.46 and NGC 7635.

As an illustrative example, we show in Figure 5 (left panel) the spectra corresponding to the SE clump of G79.29+0.46. We can distinguish three velocity

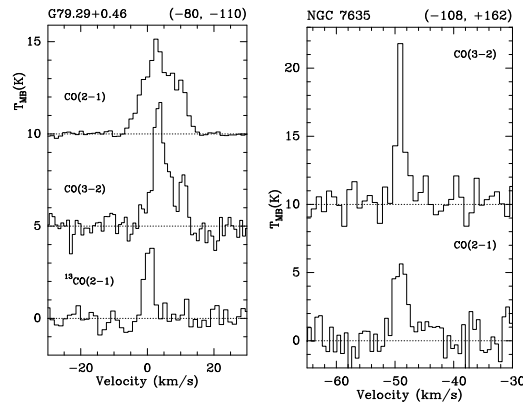


Figure 5: Observed spectra at prominent clumps, located in the fields of G79.29+0.46 (left) and NGC 7635 (right). We can see important differences among the observed lines, indicating different excitation conditions depending on the velocity range considered.

ranges. For velocities between -3 and $+3$ km s^{-1} , the low CO 2–1 / ^{13}CO 2–1 line ratio talks about a high opacity of the CO lines. For velocities around 10 km s^{-1} , the high CO 3–2 / CO 2–1 line ratio indicates a higher density. For intermediate velocities, the relative intensities are compatible with general galactic clouds. Similar differences are noted in the case of NGC 7635 (Figure 5, right panel).

5 Conclusions and future prospects

The interplay between the massive stars and the interstellar medium is fairly well established for the main sequence and the W-R stages. However, little is known for the intermediate evolutive phases, when the most violent and fast mass ejections occur. In NGC 2359, the mass loss history of the W-R progenitor was reconstructed by “reading” the imprints produced by the star onto its surrounding gas [15]. As a result, a previous LBV phase appeared as responsible of several shocked layers, clearly detected in CO and other molecules. On the other hand, recent numerical simulations [5] predict densities for the compressed gas high enough to allow the survival and the formation of molecules.

In this study we have searched for the molecular signatures around already known

ring nebulae and disks around a sample of evolved, pre-WR stars. In most of the cases, a significant amount of CO has been detected, located beyond the ionized and/or atomic gas. The *minimum* densities inferred are well above 10^4 cm^{-3} , which can only be explained in such a harsh environment by the action of a compressing agent, such as the variable stellar winds and mass ejections. Local variations of the CO opacity may also indicate important inhomogeneities in the physical parameters.

The local conditions where this molecular gas has been detected are extremely hostile for the survival of molecules, both because of the high UV field (in some cases, up to 10^6 times the mean galactic UV field) and the mass-loss history of the massive star. So far, this kind of studies is worth to be continued, in order to better understand how common these scenarios are, how they evolve and how this affects the dynamical and chemical evolution of the Galaxy as a whole. In this sense, a set of reasonable follow-up steps are the enhancement of the sample, and the search for more complex molecules.

Acknowledgements: This work was supported by the Spanish Ministerio de Ciencia y Tecnología, under grant AYA2003-06473. The SMT is operated by the Arizona Radio Observatory (ARO), Steward Observatory, University of Arizona.

References

- [1] Weaver, R., McCray, R., Castor, J., Shapiro, P., Moore, R. 1977, ApJ 218, 377
- [2] Matzner C.D. 2002, ApJ 566, 302
- [3] Maeder, A., Meynet, G. 1994, A&A 287, 803
- [4] García-Segura, G., Mac Low, M.M., Langer, N. 1996, A&A 305, 229
- [5] van Marle, A.J., Langer, N., García-Segura, G. 2004, RMA&A Conf. Ser. 22, 136
- [6] Arnal, E.M., Cappa, C.E., Rizzo, J.R., Cichowolski, S. 1999, AJ 118, 1798
- [7] Cappa, C.E., Herbstmeier, U. 2000, AJ 120, 1906
- [8] Marston, A.P. 1996, AJ 109, 2257
- [9] Chu, Y.-H., Treffers, R.R., Kwitter, K.B. 1983, ApJS 53, 937
- [10] St. Louis, N., Doyon, R., Chagnon, F., Nadeau, D. 1998, AJ 115, 2475
- [11] Marston, A.P., Welzmilller, J., Bransford, M.A., Black, J.H., Bergman, P. 1999, ApJ 518, 769
- [12] Rizzo, J.R., Martín-Pintado, J., Mangum, J.G. 2001, A&A 366, 146
- [13] Rizzo, J.R., Martín-Pintado, J., Henkel, C. 2001, ApJ 553, L181
- [14] Rizzo, J.R., Martín-Pintado, J., Desmurs, J.-F. 2002, IAU Symp 212, 742
- [15] Rizzo, J.R., Martín-Pintado, J., Desmurs, J.-F. 2003, A&A 411, 465
- [16] Morris, P.W. 2000, in *ISO beyond the peaks*, ESA-SP, 456, 165
- [17] Ueta, T., Meixner, M., Dayal, A., Deutsch, L.K., Fazio, G., Hora, J., Hoffmann, W.F. 2001, ApJ 548, 1020

- [18] Clark, J.S., Egan, M.P., Crowther, P.A., Mizuno, D.R., Larionov, V.M., Arkahrov, A. 2003, *A&A* 412, 185
- [19] Eikenberry, S.S., Matthews, K., LaVine, J.L., et al. 2004, *ApJ* 616, 506
- [20] Miroshnichenko, A.S., Fremat, Y., Houziaux, L., Andrillat, Y., Chentsov, E.L., Klochkova, V.G. 1998, *A&AS* 131, 469
- [21] Higgs, L.A., Wendker, H.J., Landecker, T.L. 1994, *A&A* 291, 295
- [22] Voors, R.H.M., Geballe, T.R., Waters, L.B.F.M., Najarro, F., Lamers, H.J.G.L.M. 2000, *A&A* 362, 236
- [23] Waters, L.B.F.M., Izumiura, H., Zaal, P.A., Geballe, T.R., Kester, D.J.M., Bontekoe, T.R. 1996, *A&A* 313, 866
- [24] Moore, B.D., Walter, D.K., Hester, J.J., Scowen, P.A., Dufour, R.J., Buckalew, B.A. 2002, *ApJ* 124, 3313
- [25] Christopoulou, P.E., Goudis, C.D., Meaburn, J., Dyson, J.E., Clayton, C.A. 1995, *A&A* 295, 509